CONF-950820--2
SAND95-1193C

# Tuning a Double Quantum Well Fermi Surface with In-Plane Magnetic Fields

J. A. Simmons, N. E. Harff, T. M. Eiles, S. K. Lyo, and J. F. Klem

Sandia National Laboratories

Albuquerque, New Mexico 87185-1415 USA



## Abstract

A double quantum well (QW) subject to in-plane magnetic fields $B_{\|}$ has the dispersion curves of its two QWs shifted in k-space. When the QWs are strongly coupled, an anticrossing and partial energy gap occur, yielding a tunable multi-component Fermi surface. We report measurements of the resultant features in the conductance, the capacitive density of states, and giant deviations in the cyclotron effective masses.

## DISCLAIMER

Double quantum wells (DQWs) constitute a system in which an additional degree of freedom can be controllably introduced to a two dimensional electron gas by changing the thickness and height of the grown interwell barrier. In the case of purely in-plane fields $B_{||}$, single particle tunneling dynamics dominate the interactions, with the primary effect of $B_{||}$ being a linear transverse shift in the momenta $\hbar\mathbf{k}$ of electrons in one QW relative to those in the other [1,2].

Here we describe our studies of a strongly coupled DQW subject to a high $B_{||}$. The strong tunneling causes the shifted QW dispersion curves to distort into an anticrossing, opening a partial energy gap or minigap. The presence of the gap mixes the two (displaced) QW Fermi circles to produce a Fermi surface (FS) with orbits of greatly differing area. At the edges of the gap, van Hove singularities in the density of states $D(\varepsilon)$ appear, and the electron group velocities approach zero. By sweeping $B_{||}$, the FS can be tuned and the gap can be made to pass through the chemical potential $\mu$, with the gap edges producing dramatic effects in the transport properties [3,4]. These include sharp features in both the conductance and the capacitance as a function of $B_{||}$, and giant deviations in the cyclotron mass $m_c$.

The two samples studied were grown by MBE. Sample *A* (*B*) consisted of a modulation-doped pair of GaAs QWs of equal width $w$ = 150 Å (100 Å) separated by an $Al_{0.3}Ga_{0.7}As$ barrier of thickness $t$ = 25 Å (35 Å). Each QW had density $n \approx 1.5 \times 10^{11}$ ($1.2 \times 10^{11}$) $cm^{-2}$ as measured by Shubnikov-de Haas oscillations (SdHO) for $B_{||}$=0. Top and bottom QW mobilities were ~2.7 and ~2.2 x $10^5$ (~1.2 and ~0.6 x $10^5$) $cm^2/Vs$. Four-terminal 17 Hz lock-in measurements were performed on Hall bars with Cr/Au top gates. Measurements of $m_c$ required a simultaneous small $B_\perp$ and large $B_{||}$, achieved by applying a uniform total field $B_T$ at angles $\theta$ = 0.0°, 2.5°, 3.0°, and 3.5° from parallel, with

rotations performed *in situ*.

In Fig. 1(a) we show the normalized in-plane resistance $R_{||}(B_{||})$ for sample *A*, at $T$=0.5 K and $\theta$=0. A minimum occurs at 5.9 T, followed by a maximum at 6.5 T. We now briefly discuss the origin of these two features [3,4]. Shown in Fig. 2(a) is a tight-binding calculation for sample *A* of the DQW dispersion $\varepsilon(k_y)$, for $B_{||}$=7.5 T in the *x*-direction [5]. $B_{||}$ shifts the two QW dispersion curves relative to one another by an amount $\Delta k_y = edB_{||}/\hbar$. The strong QW coupling produces an anticrossing and minigap whose width $\varepsilon_G$ (of order 1 meV) is independent of $B_{||}$ and $\approx \Delta_{SAS}$, the zero-field symmetric-antisymmetric gap [6]. The minigap dramatically distorts $D(\varepsilon)$ and the electron group velocities [Fig. 2(b)]. Since the upper branch of $\varepsilon(\mathbf{k})$ is nearly parabolic, a step-like increase occurs in $D(\varepsilon)$ at the upper gap edge. Thus as $B_{||}$ is increased and the gap moves upward, the (low velocity) states at the upper gap edge pass through $\mu$ and are abruptly emptied, reducing the scattering and causing a sharp minimum in $R_{||}$. By contrast, $\varepsilon(\mathbf{k})$ at the lower gap edge is saddle-shaped, yielding a logarithmic divergence in $D(\varepsilon)$. When $B_{||}$ is further increased and the lower gap edge crosses $\mu$, electrons are divergently scattered into these (zero-velocity) states, yielding the sharp maximum in $R_{||}$.

The shape of the FS is determined by the intersection of $\mu$ and $\varepsilon(\mathbf{k})$. For $B_{||} < 5.9$ T, $\mu$ lies above the gap and the FS has a small lens-shaped orbit lying within a larger hourglass-shaped orbit, shown in Fig. 2(c). For 5.9 T $< B_{||} <$ 6.5 T, $\mu$ lies in the gap and only the hourglass orbit is present. As $B_{||}$ is increased further, $\mu$ touches the lower gap edge, causing the hourglass "waist" to pinch off. For $B_{||} > 6.5$ T, the FS separates into two Fermi circles of roughly equal size.

Changes $\Delta D(\varepsilon)$ in $D(\varepsilon)$ can be measured directly via changes $\Delta C(B_{||})$ in the capacitance between the surface gate and the DQW. For $\Delta D(\varepsilon)$ small relative to the full 2D

density of states, $\Delta C(B_{||}) \propto \Delta D(\varepsilon)$ [7]. This condition appears to hold for our sample, based on a calculation of the geometrical capacitance. In Fig. 3 we show $\Delta C(B_{||})$ of sample *B* (gate area ~5.4 mm$^2$) for several different gate voltages. In contrast to the conductance data, $C(B_{||})$ remains relatively constant at low B||, until a sudden step-like decrease appears. This corresponds to the disappearance of the lens orbit, occuring when the upper gap edge crosses $\mu$. $C(B_{||})$ then increases monotonically, and ends in a slight peak before settling at a value nearly the same as just before the step-decrease. The peak is due to the lower gap edge, with a logarithmic singularity in D(E), crossing $\mu$, and is washed out due to damping. The relative constancy of $C(B_{||})$ outside the anticrossing region is in stark contrast to $R_{||}$ [see Fig. 1(a)], which convolves the changing Fermi velocities. The overall shape of $C(B_{||})$ bears a striking resemblance to the calculated $D(\varepsilon)$ of Fig. 2(b). The slight oscillations just below the step-decrease are SdHO due to a slight misalignment of the sample from $\theta$=0, which brings us to our next topic.

By adding a small $B_\perp$ and measuring the temperature ($T$) dependence of the resulting (SdHO), we probed $m_c$ near the minigap [8]. $B_{||}$ and $B_\perp$ could not be swept independently, mixing the SdHO with the anticrossing features. To remove this mixing, for each $T$ examined we subtracted the resistance at $\theta$=0 [e.g. Fig. 1(a)] from the resistance in a tilted field, to yield $\Delta R(B_{||},\theta) = R(B_{||},\theta) - R(B_{||},\theta=0)$. Fig. 1(b) shows $\Delta R(B_{||},\theta=3.0^\circ)$ for several $T$. The SdHO are uniform up to ~5.9 T; then both the period and amplitude change significantly, indicating a drastic change in $m_c$. To determine $m_c$ from the $T$-dependence of the SdHO, we first consider which FS orbits contribute. For $B_{||}$ < 5.9 T, the lens and hourglass orbits enclose greatly different areas in **k**-space. Electrons traverse these orbits at a rate $d\mathbf{k}/dt = -(e/\hbar)\mathbf{v_k} \times \mathbf{B}_\perp$, where $\mathbf{v_k}$ is the Fermi velocity. When $\theta$ and hence $B_\perp$ are sufficiently small, electrons in the hourglass are unable to complete the

orbit without scattering, contributing negligibly to the SdHO. However, because $\mathbf{v_k}$ is nearly the same for the two orbits (except very close to the gap edge), enough electrons complete the lens orbit to produce SdHO. This assumption agrees with the data for $B_{\|} <$ 5.9 T, where only a single period occurs for all three θ. For 5.9 T < $B_{\|}$ < 6.5 T, the FS consists of only the hourglass, while for $B_{\|} >$ 6.5 T, the FS consists of two separated Fermi circles of equal size, producing SdHO of the same period and $T$-dependence. Thus for all three ranges, the SdHO arises from a single orbit of the FS.

For a single FS orbit, the SdHO are in general described by a series of terms [9]. However when $B_{\perp}$ is small enough that $\omega_c\tau$ is of order unity (where $\omega_c = eB_{\perp}/m_c$, and $\tau$ is the scattering time), the higher order terms become negligible and the SdHO become small in amplitude and sinusoidal in shape. This is in accord with our data, where the oscillations are strongly sinusoidal and never exceed 15% of the background. When higher order terms are negligible, the SdH amplitude is given by

$$\frac{\delta R(T)}{\delta R(T_0)} = \frac{T\sinh(\beta T_0(m_c/m_0)/B_{\perp})}{T_0\sinh(\beta T(m_c/m_0)/B_{\perp})} \qquad (1)$$

where $T_0$ is base $T$, $\beta = 2\pi^2 k_B m_0/\hbar e$, and $m_0$ is the free electron mass. Fig. 1(b) inset shows two typical fits of Eq. (1) to the θ = 3.0° data. (Here $\delta R$ is obtained by taking the difference between $\Delta R(B_{\|},\theta)$ evaluated at adjacent SdHO extrema, and subtracting the magnetoresistance background.) While for 8.49 T $m_c = 0.070\ m_0$, for 5.09 T $m_c = 0.025$ $m_0$, a factor of three lower than $m^*_{GaAs}$. In general, the fits yield $m_c$ to ± 10% error. For the range ~5.9 ≤ $B_{\|}$ ≤ ~6.5 T, however, $m_c$ is changing rapidly, yielding larger errors of roughly ± 20%.

Fig. 4 shows $m_c(B_{\|})$ for all three θ. At 2.7 T, $m_c \approx 0.050\ m_0$, considerably lower than $m^*_{GaAs}$. Raising $B_{\|}$ causes $m_c$ to decrease, reaching 0.021 $m_0$ near the upper gap

edge at 5.6 T. As $B_{||}$ is increased further, $m_c$ suddenly increases, reaching a value of 0.099 $m_0$ just below 6.5 T, where $\mu$ crosses the lower gap edge, or saddle point. $m_c$ then rapidly converges to $m^*_{GaAs}$ near ~7 T and remains roughly constant thereafter.

Following Lyo [10], an understanding of the behavior of $m_c$ can be gained by examining Fig. 2 and employing the expression $m_c = (\hbar/2\pi)\oint \mathbf{v}_k^{-1} d\mathbf{k}$, where the integration is along the dominant orbit. As $B_{||}$ is increased, the upper gap edge moves upward towards $\mu$. As a result, the size of the lens orbit decreases, while $\mathbf{v}_k$ decreases more slowly, resulting in a monotonic decrease of $m_c$. The lens orbit vanishes at 5.9 T, but because $\mathbf{v}_k$ also vanishes, $m_c$ does not go to zero. Above 5.9 T, the orbit size increases abruptly as electrons move to the hourglass, causing an abrupt increase in $m_c$. As $B_{||}$ increases from 5.9 to 6.5 T, $\mu$ lies in the minigap and moves towards the saddle point. At the same time, $\mathbf{v}_k$ becomes smaller near the saddle-point, yielding now a monotonic *increase* of $m_c(B_{||})$. The divergence of $m_c$ at the saddlepoint, due to $\mathbf{v}_k$ vanishing, is suppressed in the data by damping. Above 6.5 T, $\mu$ falls below the saddle point, causing the hourglass to split into two roughly circular orbits with nearly parabolic dispersion. The two QWs are thus effectively uncoupled, and $m_c$ approaches $m^*_{GaAs}$. In Fig. 4 we plot Lyo's calculation of $m_c(B_{||})$ for sample *A*, where $B_{||}$ has been scaled by 0.96. Excellent agreement is seen.

In summary, an anticrossing and minigap appear in strongly coupled DQWs subject to a strong $B_{||}$. These give rise to singularities in the density of states, sharp features in the in-plane resistance and the gate capacitance, and giant deviations in the cyclotron effective masses. This work was supported by the U. S. Dept. of Energy under Contract No. DE-AC04-94AL85000.

## References


[1] J.P. Eisenstein. T.J. Gramila, L.N. Pfeiffer, and K.W. West, Phys. Rev. B **44,** (1991) 6511.

[2] J.A. Simmons, S.K. Lyo, J.F. Klem, M.E. Sherwin, and J.R. Wendt, Phys. Rev. B **47**, (1993) 15 741; S.K. Lyo and J.A. Simmons, J. Phys.: Condens. Matter **5**, (1993) L299.

[3] J.A. Simmons, S.K. Lyo, N.E. Harff, and J.F. Klem, Phys. Rev. Lett. **73**, (1994) 2256.

[4] S.K. Lyo, Phys. Rev. B **50**, (1994) 4965.

[5] Including the Hartree term increases the center-to-center distance between the wavefunctions of the two QWs, thus lowering the $B_{||}$ at which the minigap crosses $\mu$, and reducing $\varepsilon_G$.

[6] G.S. Boebinger, H.W. Jiang, L.N. Pfeiffer, and K.W. West, Phys. Rev. Lett. **64**, (1990) 1793.

[7] M. Buttiker, J. Phys.: Condens. Matter **5**, (1993) 9361, and references therein.

[8] N.E. Harff, J.A. Simmons, S.K. Lyo, J.E. Schirber, J.F. Klem, and S.M. Goodnick, in The Physics of Semiconductors, Vol.1, Ed. D.J. Lockwood, (World Scientific, Singapore, 1995) p. 831.

[9] T. Ando, A.B. Fowler, and F. Stern, Rev. Mod. Phys. **54**, (1982) 437.

[10] S.K. Lyo, Phys. Rev. B **51**, (1995) 11 160.

## Figure Captions

FIG. 1. (a) Normalized $R_{||}(B_{||})$ of sample A at $\theta$=0. (b) $\Delta R(B_{||},\theta=3.0°)$ for several T. Inset: SdHO amplitudes vs. $T$, and fits to Eq. (1) for two $B_{||}$.

FIG. 2. Sample $A$ calculations at $B_{||}$ = 7.5 T. (a): $\varepsilon(k_y)$ with (solid lines) and without (dotted lines) coupling. (b): $D(\varepsilon)$ for lower energy branch (dotted line) and both branches (solid line). (c): Fermi surface sketch for $\mu \approx 9$ meV.

FIG. 3. Change in capacitance $\Delta C(B_{||})$, proportional to $\Delta D(\varepsilon)$, for several gate biases. The curves are strikingly similar to Fig. 2(b).

FIG. 4. Summary of measured $m_c$ values vs. $B_{||}$. Solid line is theoretical calculation of Ref. [10].

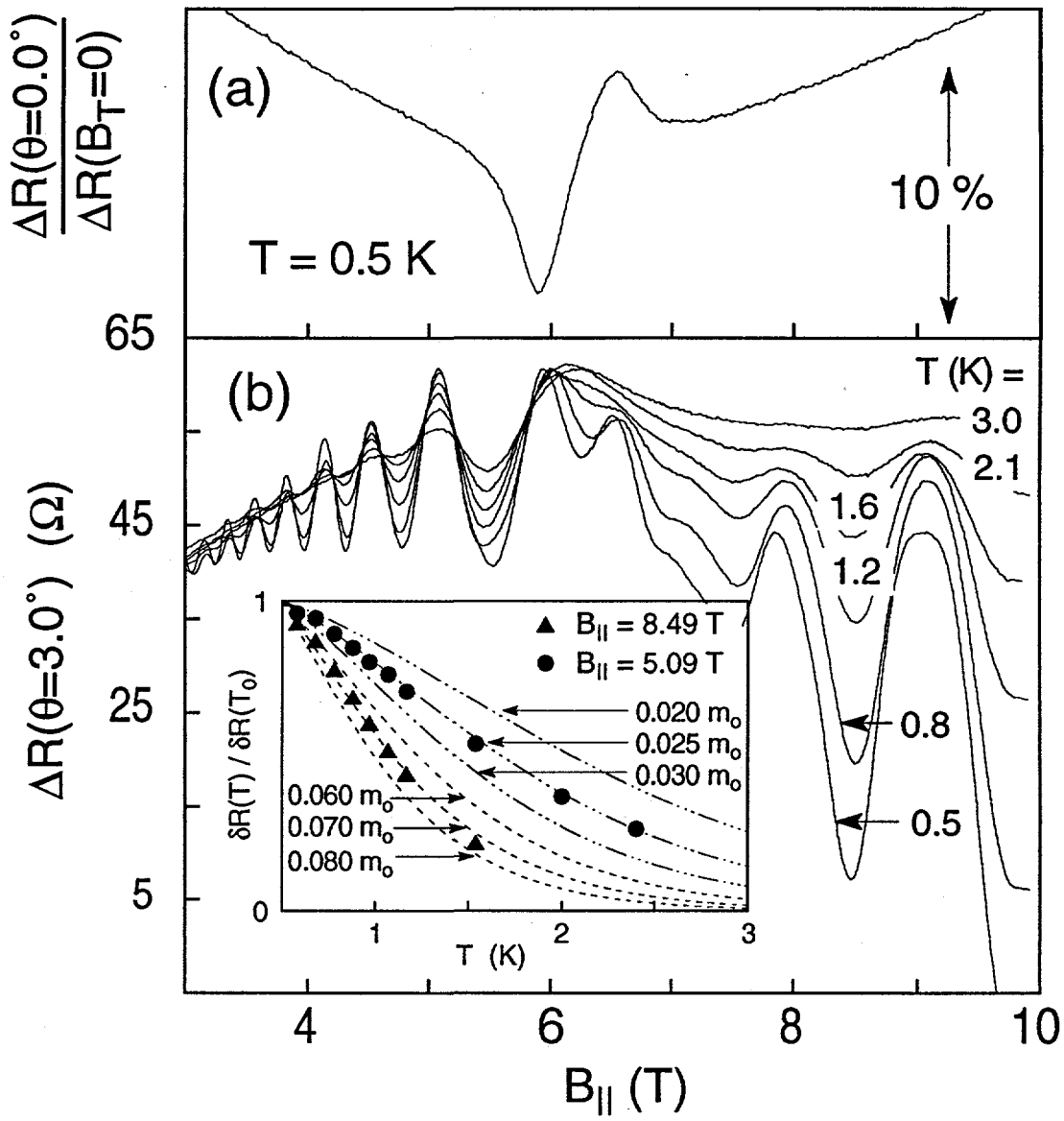
(a)
T = 0.5 K
10 %
(b)
T (K) =
3.0
2.1
1.6
1.2
0.8
0.5
$\frac{\Delta R(\theta=0.0^\circ)}{\Delta R(B_T=0)}$
$\Delta R(\theta=3.0^\circ)$ (Ω)
65
45
25
5
4
6
8
10
$B_{||}$ (T)
$B_{||}$ = 8.49 T
$B_{||}$ = 5.09 T
0.020 $m_o$
0.025 $m_o$
0.030 $m_o$
0.060 $m_o$
0.070 $m_o$
0.080 $m_o$
$\delta R(T) / \delta R(T_o)$
T (K)
1
0
1
2
3

FIG. 1

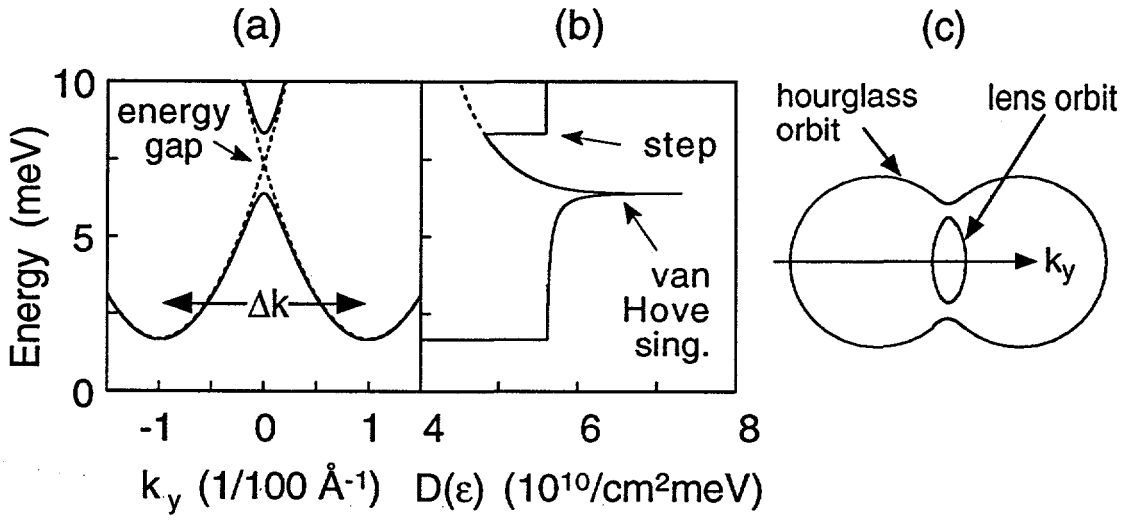
(a)
(b)
(c)
10
5
0
Energy (meV)
energy gap
Δk
step
van Hove sing.
hourglass orbit
lens orbit
$k_y$
-1
0
1
4
6
8
$k_y$ (1/100 Å$^{-1}$)
D(ε) (10$^{10}$/cm$^2$meV)

FIG. 2

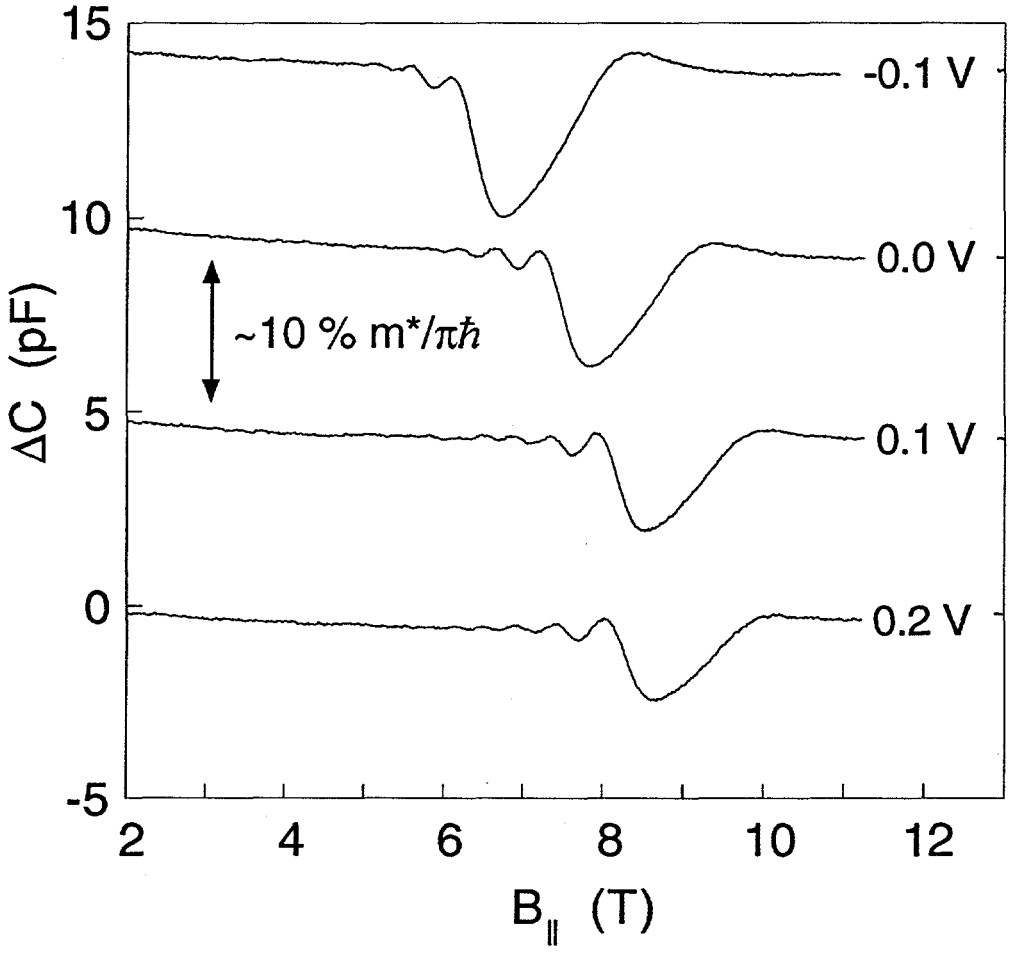


FIG. 3

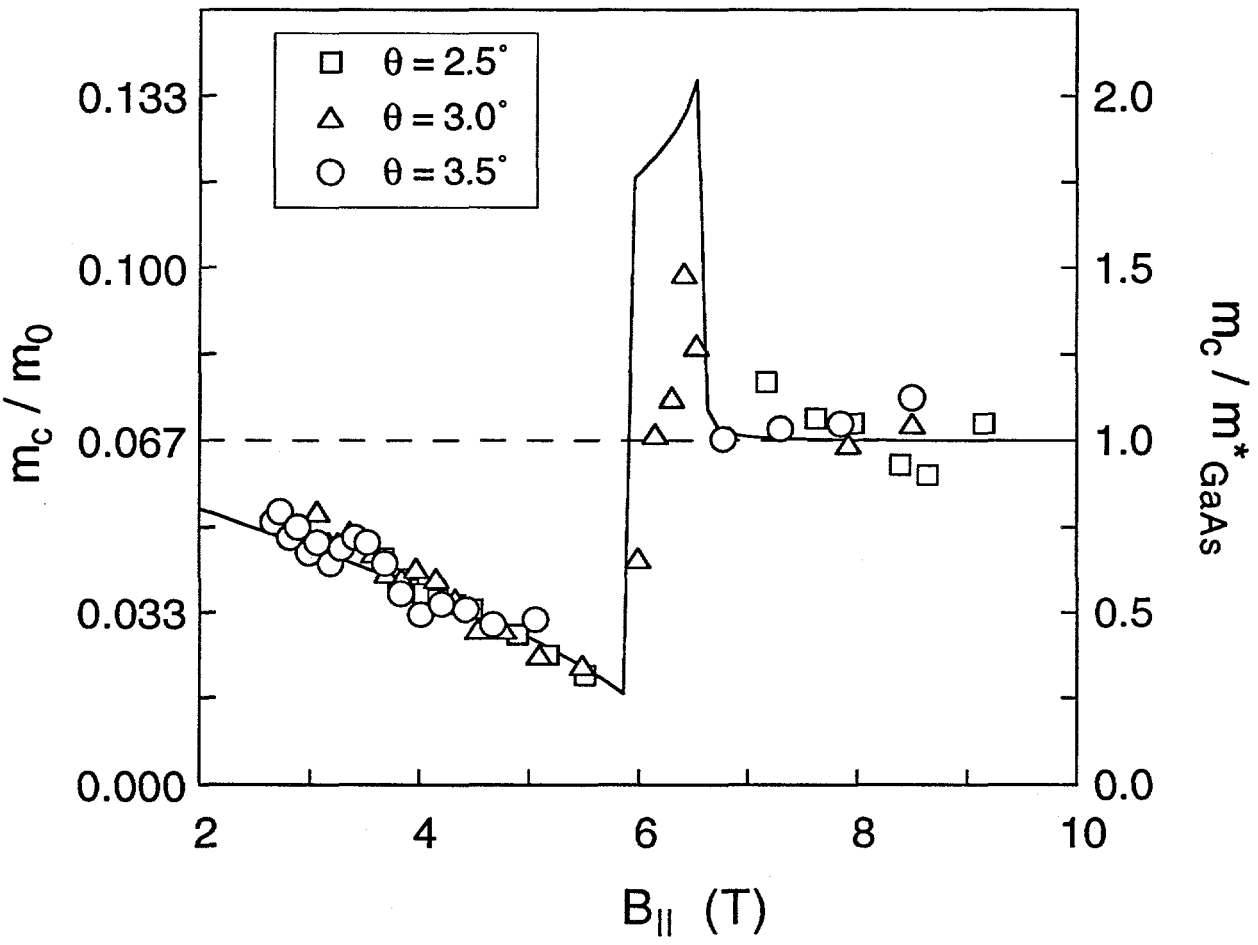
θ = 2.5°
θ = 3.0°
θ = 3.5°
0.133
0.100
0.067
0.033
0.000
2.0
1.5
1.0
0.5
0.0
2
4
6
8
10
$m_c / m_0$
$m_c / m^*_{GaAs}$
$B_{||}$ (T)

FIG. 4